Search for the Decay $\pi^0 \rightarrow \gamma + X$

M. S. Atiya, I-H. Chiang, J. S. Frank, J. S. Haggerty, M. M. Ito,[a] T. F. Kycia, K. K. Li, L. S. Littenberg, A. J. Stevens, A. Sambamurti,[b] and R. C. Strand
Brookhaven National Laboratory, Upton, New York 11973

W. C. Louis
Medium Energy Physics Division, Los Alamos National Laboratory, Los Alamos, New Mexico 87545

D. S. Akerib,[c] D. R. Marlow, P. D. Meyers, M. A. Selen,[d] F. C. Shoemaker, and A. J. S. Smith
Joseph Henry Laboratories, Princeton University, Princeton, New Jersey 08544

E. W. Blackmore, D. A. Bryman, L. Felawka, P. Kitching, A. Konaka, Y. Kuno,[e] J. A. Macdonald, T. Numao, P. Padley, J-M. Poutissou, R. Poutissou, J. Roy, and A. S. Turcot
TRIUMF, Vancouver, British Columbia, Canada V6T 2A3
(Received 27 February 1992)

A search for the decay $\pi^0 \rightarrow \gamma X$, where X is any long-lived weakly interacting neutral vector particle with mass smaller than the neutral pion mass, was performed using neutral pions tagged by $K^+ \rightarrow \pi^+ \pi^0$. A 90%-C.L. upper limit for the branching ratio of the two-body decay $B(\pi^0 \rightarrow \gamma X) < 5 \times 10^{-4}$ is set. Limits are also set for three-body decays $\pi^0 \rightarrow \gamma X X'$.

PACS numbers: 13.40.Hq, 14.80.Er

In this Letter we report the first experimental upper limit on the branching ratio for the exotic decay $\pi^0 \rightarrow \gamma X$, where X is a hypothetical long-lived neutral noninteracting particle. Owing to angular momentum conservation, observation of such a signal would indicate the unambiguous existence of a new *vector* particle [1]. The experiment is sensitive to the mass region $0 \leq m_X < m_{\pi^0}$, where m_{π^0} is the neutral pion mass. The possibilities for X include a new light gauge boson [2,3] which appears in some extensions of the standard model with an additional U(1) interaction [4], or an "axigluon" [5]. The present search is also sensitive to three-body decays $\pi^0 \rightarrow \gamma X X'$, where X and X' could be particles such as neutrinos [6] or supersymmetric particles [2].

This experiment is similar to a search for the rare decay $\pi^0 \rightarrow \nu\bar{\nu}$ previously reported [7]. A π^0 was tagged by the 205-MeV/c π^+ accompanying it in $K^+ \rightarrow \pi^+ \pi^0$ decay of stopped kaons. The signature of $\pi^0 \rightarrow \gamma X$ decay is a positive pion kinematically consistent with $K^+ \rightarrow \pi^+ \pi^0$ decay, accompanied by a single photon. The principal source of potential background is $\pi^0 \rightarrow \gamma\gamma$ decay where one photon escapes undetected. To minimize this background, it is critical to have a hermetic photon detector with high detection efficiency.

The experiment was performed using the low-energy-separated beam (LESBI) at the Alternating Gradient Synchrotron at Brookhaven National Laboratory. The cylindrically symmetric detector, whose side and end views are shown in Fig. 1, was designed primarily to search for $K^+ \rightarrow \pi^+ \nu\bar{\nu}$, and is described in more detail in Ref. [1] and references therein. A 775-MeV/c K^+ beam was slowed by a BeO degrader and stopped in a segmented scintillating-fiber target located at the center of the detector. Charged decay products were momentum analyzed in a cylindrical drift chamber in a 1-T axial magnetic field. After traversing the drift chamber they were stopped in a fifteen-layer scintillator range stack that surrounded the drift chamber. These counters were used to measure kinetic energy and range. The range-stack scin-

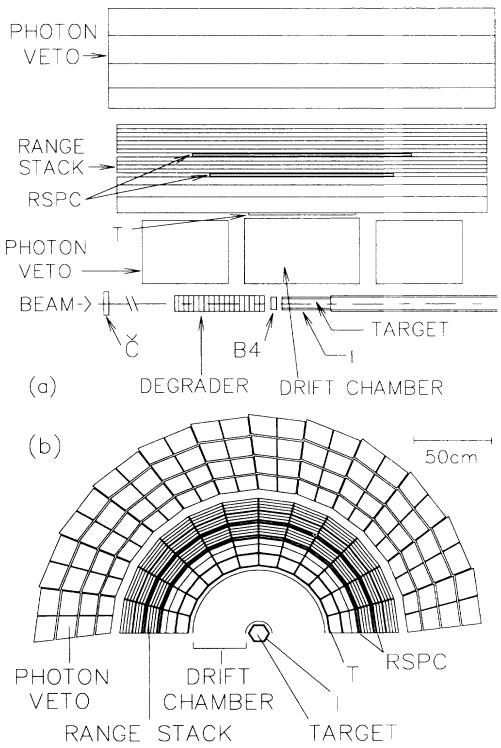

FIG. 1. Schematic (a) side and (b) end views of the upper half of the detector.

tillators were instrumented with transient digitizers (TDs) which recorded phototube pulse heights with an 8-bit dynamic range every 2 ns. The TD pulse-shape information was used to identify pions through their characteristic $\pi^+ \to \mu^+ \to e^+$ decay sequence.

Photons were detected in an electromagnetic barrel calorimeter that surrounded the range stack, in the range stack itself, and in a pair of end-cap calorimeters located upstream and downstream of the drift chamber. The calorimeters consisted of alternating layers of 1-mm lead and 5-mm scintillator and covered a solid angle of almost 4π. In the barrel calorimeter, the 2-m-long plastic scintillators were viewed by phototubes at each end. The barrel calorimeter had 48-fold azimuthal and 4-fold radial segmentation; the end caps and range stack had 24-fold azimuthal segmentation. The barrel, range-stack, and end-cap arrays had total thicknesses of 14, 1, and 12 r.l. (radiation lengths), respectively. The energy resolution of the calorimeters was approximately $\sigma_E/E = 8\%/\sqrt{E}$ (E in GeV).

$K^+ \to \pi^+\pi^0$ data were selected by a trigger that required a charged track to stop in the region of the range stack between 8 and 35 cm of scintillator in order to remove $K^+ \to \mu^+\nu$ and $K^+ \to 3\pi$ decays. About 40% of the total $K^+ \to \pi^+\pi^0$ data used in the present analysis had additional requirements imposed on-line by two higher level triggers. The first level required that the total additional energy in the range stack not associated with the track of a charged particle be less than 12 MeV (extra-energy cut). This requirement eliminated events with photons showering in the range stack, thereby simplifying subsequent stages in the off-line analysis. The second level trigger analyzed the TD pulse-shape data from the stopping layer to distinguish pions from muons by looking for evidence of a second pulse arising from $\pi^+ \to \mu^+\nu$ decay following the stopping pulse. For the remaining 60% of the data that were not subject to the on-line trigger constraints, these two additional requirements were imposed off-line during analysis. In addition, in-flight K^+ decays were eliminated from the full data set by requiring the kaon decay time to be at least 2 ns later than the kaon stopping time.

The analysis was divided into two parts: π^0 tagging, and selection of events with only one photon which was required to have converted in the barrel calorimeter. Tagged π^0's from well-defined $K^+ \to \pi^+\pi^0$ samples were selected by requiring exactly one positive charged track in the target, in the drift chamber, and in the range stack with satisfactory spatial matching at the boundaries. To identify a pion and eliminate $K^+ \to \mu^+\nu$ (γ) and $K^+ \to \mu^+\pi^0\nu$ decays, the TD information was used to reconstruct the decay sequence of $\pi^+ \to \mu^+ \to e^+$, as described in Ref. [1]. Next, the relationship between momentum and range was required to be consistent with that of a charged pion. Finally, kinematic cuts were placed on momentum, kinetic energy, and range of the charged track, demanding that they be consistent with the 205-MeV/c π^+ from $K^+ \to \pi^+\pi^0$ decay within 3σ of the resolution in each parameter. The resolutions of momentum, kinetic energy, and range for $K^+ \to \pi^+\pi^0$ decay were 2.7%, 3.8%, and 3.9%, respectively. A total of 87077 $K^+ \to \pi^+\pi^0$ events was selected. The only significant potential source of background that could survive the selection process was pion scattering from the incident beam, estimated to be $< 1\%$.

In the second part of the analysis, events were sought with a single-photon cluster in the barrel calorimeter and no photons in any other detector subsystems including the end-cap calorimeter, range stack, and target. This condition also eliminated $\pi^0 \to \gamma e^+ e^-$ decay. In the range stack and target, hit elements associated with the π^+ track were excluded from the search for photon energy. The extra-energy cut in the on-line trigger selection contained part of the photon selection for the 40% of the data discussed above. The number of tagged π^0's from this portion of the data was corrected to account for this photon selection before tagging to give an effective total number of observed π^0's of $N_{\pi^0} = 139243$.

To be counted as photon energy, pulses in the barrel were required to have a leading-edge time in a window from -6 to $+14$ ns with respect to the K^+ decay time. The asymmetric time window was used to include the slow products of photonuclear interactions. Adjacent struck modules were considered to be associated with a single-photon shower. For each hit module the hit position in the plane perpendicular to the detector (beam) axis was determined by the azimuthal and radial segmentation of the calorimeter. The hit position along the detector axis was calculated from end-to-end time and pulse-height differences. The location of the photon shower was then obtained by an energy-weighted average of the hit positions of all modules belonging to the shower. Events were kept with either one photon cluster or with more than one cluster provided that the visible energy of the second largest cluster was less than 0.3 MeV. For the other detector subsystems, the photon-veto thresholds were 0.3, 1, and 2 MeV in visible energy for the end-cap calorimeter, range stack, and target, respectively.

At this stage of analysis the surviving events were predominantly due to $\pi^0 \to \gamma\gamma$ decay with the two photons hitting the same (or adjacent) barrel calorimeter modules at different positions along the dimension parallel to the detector axis. Owing to momentum conservation, events of this type have the photon cluster located at 180° to the π^+ track with respect to the K^+ decay vertex in the plane perpendicular to the detector axis. To eliminate this background, two cuts were applied. The first required that the azimuthal opening angle between the photon and the π^0 direction inferred from the π^+ be greater than 20°. This kinematic cut also effectively eliminated background $\pi^0 \to \gamma\gamma$ events where the lower-energy pho-

ton overlayed the π^+ track, where the photon had the highest likelihood of being missed. Second, since these events are characterized by a single-photon cluster with energy close to the total π^0 energy of $E_{\pi^0}=245$ MeV in $K^+\to\pi^+\pi^0$ decay, events with photon energy greater than 150 MeV were removed.

After all cuts, eight events survived, none of which showed any evidence of being due to beam pion scattering. For those events, the missing mass squared m_X^2 was calculated using energies and momenta of the observed photon and the π^0 (determined from the observed π^+). Figure 2 shows the distribution of m_X^2 for the remaining events along with the expected mass-squared resolution for $m_X=0$ MeV/c^2. These surviving events were consistent with $\pi^0\to\gamma\gamma$ events expected with one photon missing due to photon detection inefficiency. A Monte Carlo (MC) simulation predicted fifteen events for this type of background. The MC study indicated that a photon was missed due either to sampling fluctuations (for low-energy photons) or to photonuclear interactions in which the reaction products were not detected (for high-energy photons). However, it is noted that the calculation is strongly dependent on the assumptions for nuclear excitation and decay after photonuclear interactions.

Because the MC calculation is too uncertain to allow us to confidently assign the observed events to background, the number of surviving events without background subtraction is used to give upper limits. To calculate the 90%-confidence-limit (C.L.) counts $N_{90}(m_X)$, the surviving events in Fig. 2 were summed within $\pm 2\sigma$ from m_X^2, where σ is the expected Gaussian mass-squared resolution for a particular value of m_X. The 90%-C.L. upper limit of the branching ratio for $\pi^0\to\gamma X$ for given m_X is

$$B(\pi^0\to\gamma X)<\frac{N_{90}(m_X)}{N_{\pi^0}\varepsilon(m_X)\varepsilon_{2\sigma}}, \quad (1)$$

where $\varepsilon(m_X)$ is the acceptance for m_X and $\varepsilon_{2\sigma}=0.9454$ is the acceptance of a $\pm 2\sigma$ peak integration. The contributions to acceptance loss reflected in $\varepsilon(m_X)$ fall into four major categories: (1) acceptance loss due to restricting valid photon conversions to the barrel calorimeter, including geometrical loss and loss by photon conversion before reaching the barrel; (2) acceptance loss due to kinematic factors, including the opening angle and photon energy cuts described above; (3) acceptance loss due to disruption of the π^+ selection by a photon from $\pi^0\to\gamma\gamma$ or $\pi^0\to\gamma X$ decay; and (4) acceptance loss due to accidental hits causing false vetoing of events. These are shown in Table I for $m_X=20$ MeV/c^2. Loss due to photon conversion was determined from MC simulation, and tested by comparing the rejection for MC-produced $K^+\to\pi^+\pi^0$ data with that for real data. The acceptance loss due to the kinematics cuts and that due to photon disruption of the π^+ analysis was also determined from MC calculation. The latter factor is greater than unity because the denominator of Eq. (1), consisting primarily of two-photon events, suffers greater disruption than the numerator. The acceptance loss due to accidentals was evaluated by applying the photon cuts to $K^+\to\mu^+\nu$ samples. The branching-ratio limits obtained for $\pi^0\to\gamma X$, typically $<5\times10^{-4}$, are shown as a function of m_X in Fig. 3 by the solid curve for the case in which X is noninteracting and stable.

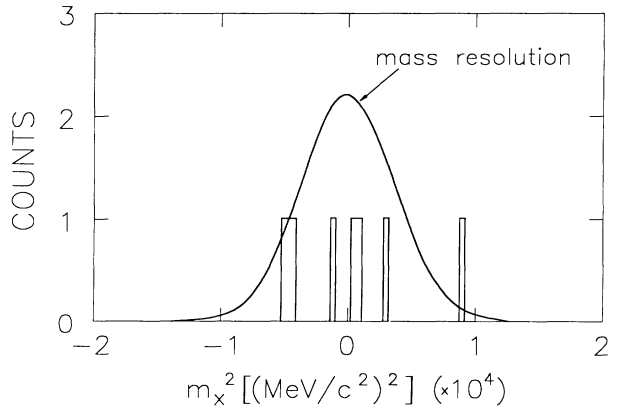

FIG. 2. Invariant missing mass squared for the surviving eight events. The solid line shows the Monte Carlo–expected mass-squared resolution for $m_X=0$ MeV/c^2.

TABLE I. Acceptance factors for $\pi^0\to\gamma X$ with $m_X=20$ MeV/c^2.

Category	Acceptance
One photon at barrel	0.52 ± 0.03
Opening angle cut	0.51 ± 0.02
Energy cut ($E_\gamma<150$ MeV)	0.88 ± 0.04
Disruption of π^+ analysis by photon	1.09 ± 0.02
Accidental loss	0.66 ± 0.02
Net acceptance	0.17 ± 0.01

This result can be used, for example, to set a limit on the magnitude of the coupling of the hypothetical gauge boson X to the quarks,

$$g^2<3\times10^{-6}(1-m_X^2/m_\pi^2)^{-3}, \quad (2)$$

about a factor of 10 below the maximum expectation in the model described in Ref. [3].

Upper limits for X decaying to detectable particles with different lifetimes are also shown as a function of m_X in Fig. 3, assuming a 1.5-m effective thickness for the active part of the detector. For small m_X the sensitivity decreases more slowly as a function of lifetime due to the increased kinetic energy of X.

Branching-ratio limits can also be set for the three-body decay $\pi^0\to\gamma XX'$. For simplicity, the masses of X and X' were assumed to be the same, thus $0\le m_X\le m_{\pi^0}/2$. Two different spectra, phase space and Dalitz-type, were used. The latter was found by replacing the

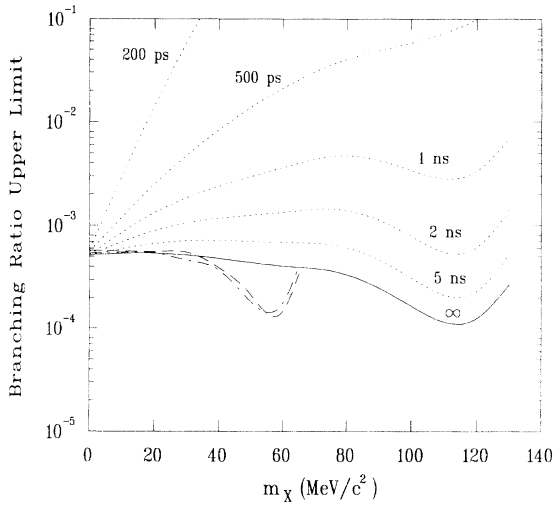

FIG. 3. The 90%-C.L. upper limits for the branching ratio of $\pi^0 \rightarrow \gamma X$ (solid curve) as a function of mass m_X. The dotted curves are the corresponding limits for finite lifetimes of X as labeled. The dot-dashed and dashed curves show the upper limit for the three-body decay $\pi^0 \rightarrow \gamma XX'$ with a phase-space spectrum and a Dalitz-type spectrum, respectively.

electron mass in the matrix element of $\pi^0 \rightarrow \gamma e^+ e^-$ decay with m_X [8]. The surviving events in Fig. 2 were integrated over several intervals, each corresponding to a range of m_X. The net acceptance was evaluated by averaging $\varepsilon(m_X)$ in each interval and taking into account the three-body spectrum. Limits (90% C.L.) for $\pi^0 \rightarrow \gamma XX'$ are shown in Fig. 3 as a function of mass m_X for the two assumed spectra and X, X' stable.

We gratefully acknowledge the dedicated efforts of the technical staffs supporting this experiment and of the Brookhaven AGS Department. This research was supported in part by the U.S. Department of Energy under Contracts No. DEAC02-76CH00016, No. W-7405-ENG-36, and No. DEAC02-76ER03072, and by the Natural Sciences and Engineering Research Council and the National Research Council of Canada.

[a]Present address: Princeton University, Princeton, NJ 08544.

[b]Deceased.

[c]Present address: California Institute of Technology, Pasadena, CA 91125.

[d]Present address: Cornell University, Ithaca, NY 14853.

[e]Present address: National Laboratory for High Energy Physics (KEK), Tsukuba, Ibaraki 305, Japan.

[1] Vector particles could also appear in other reactions such as the decay $K^+ \rightarrow \pi^+ X$. However, Glashow-Iliopoulos-Maiani suppression and helicity suppression for spin $\neq 0$ and massless X apply for $K^+ \rightarrow \pi^+ X$, whereas $\pi^0 \rightarrow \gamma X$ is not suppressed by these mechanisms. For the latest results on the search for the $K^+ \rightarrow \pi^+ a$ decay by the present experiment, see M. S. Atiya *et al.*, Phys. Rev. Lett. **64**, 21 (1990).

[2] M. I. Dobrolyubov, Yad. Fiz. **52**, 551 (1990) [Sov. J. Nucl. Phys. **52**, 352 (1990)]; M. I. Dobrolyubov and A. Yu. Ignatiev, Phys. Lett. B **206**, 346 (1988); Z. Phys. C **39**, 251 (1988); Nucl. Phys. **B309**, 655 (1988).

[3] A. E. Nelson and N. Tetradis, Phys. Lett. B **221**, 80 (1989).

[4] For hyperphoton, M. Suzuki, Phys. Rev. Lett. **56**, 1339 (1986); S. H. Aronson, H.-Y. Cheng, E. Fischbach, and W. Haxton, Phys. Rev. Lett. **56**, 1342 (1986); C. Bouchiat and J. Iliopoulos, Phys. Lett. **169B**, 447 (1986). For paraphoton, B. Holdom, Phys. Lett. **166B**, 196 (1986).

[5] F. Cuypers and P. H. Frampton, Phys. Rev. Lett. **60**, 1237 (1988); J. Bagger, C. Schmidt, and S. King, Phys. Rev. D **37**, 1188 (1988); P. H. Frampton and S. L. Glashow, Phys. Lett. B **190**, 157 (1987).

[6] L. Arnellos, W. J. Marciano, and Z. Parsa, Nucl. Phys. **B196**, 365 (1982). The standard model predicts $B(\pi^0 \rightarrow \gamma \nu \bar{\nu}) \sim 10^{-18}$.

[7] M. S. Atiya *et al.*, Phys. Rev. Lett. **66**, 2189 (1991).

[8] In principle, the limit for $\pi^0 \rightarrow \gamma XX'$ with the Dalitz-type spectrum can be used to place constraints on subminimum-ionizing particles with small fractional electric charge $\pm\epsilon$ [M. I. Dobrolyubov and A. Yu. Ignatiev, Phys. Rev. Lett. **65**, 679 (1990); S. Davidson, B. Campbell, and D. Bailey, Phys. Rev. D **43**, 2314 (1991)]. In this case, X and X' are assumed to be produced electromagnetically (proportional to ϵ^2) through a virtual photon, i.e., $\pi^0 \rightarrow \gamma\gamma^* \rightarrow \gamma X^{+\epsilon} X^{-\epsilon}$. However, since our experimental signature requires that the particles be undetected, our acceptance is limited to values of ϵ less than about 0.15. Our present statistical sensitivity for an upper limit on ϵ is insufficient to reach significantly below this acceptance cutoff.